SLIDING GAIT ALGORITHM FOR THE ALL-TERRAIN HEX-LIMBED EXTRA-TERRESTRIAL EXPLORER (ATHLETE)

Julie Townsend*
Mobility and Robotic Systems
Jet Propulsion Laboratory
California Institute of Technology
Pasadena, California 91109
Email: julie.a.townsend@jpl.nasa.gov

Jeffrey Biesiadecki
Mobility and Robotic Systems
Jet Propulsion Laboratory
California Institute of Technology
Pasadena, California 91109
Email: jeffrey.j.biesiadecki@jpl.nasa.gov

ABSTRACT

The design of a surface robotic system typically involves a trade between the traverse speed of a wheeled rover and the terrain-negotiating capabilities of a multi-legged walker. The ATHLETE mobility system, with both articulated limbs and wheels, is uniquely capable of both driving and walking, and has the flexibility to employ additional hybrid mobility modes. This paper introduces the Sliding Gait, an intermediate mobility algorithm faster than walking with better terrain-handling capabilities than wheeled mobility.

NOMENCLATURE

θ Direction of SGait step in ATHLETE Leg Frame.
Δy Component of SGait step parallel to y_L.
d_{HP} Horizontal offset between Leg Frame origin and hip pitch joint axis.
d_{step} SGait step size.
h_{reach} Horizontal limit of reachable workspace
$maxstep$ Maximum step achievable within reachable workspace.
v_{marg} Vertical extension margin for terrain variation.
v_{reach} Vertical limb extension in ATHLETE Leg Frame.
x_{min} Minimum allowable x_L.
(eN_x, eN_y) Location of step endpoint N.
(g_x, g_y) Goal position for step placement within workspace.
(x_c, y_c) Minimum clearance between steps
(x_R, y_R, z_R) Coordinate in ATHLETE Rover Frame.
(x_L, y_L, z_L) Coordinate in ATHLETE Leg Frame.
$(x_{tool}, y_{tool}, z_{tool})$ Coordinate in ATHLETE Tool Frame.

*Address all correspondence to this author.

INTRODUCTION

Wheeled mobility systems with passive suspensions have long been the standard for exploration of planetary surfaces. They are efficient and capable for driving over relatively obstacle-free surface terrain. However, even proven rovers operated by an experienced team may encounter a terrain anomaly that threatens future mobility of the system, as demonstrated by both Mars Exploration Rovers. In the course of their missions, both Spirit and Opportunity became embedded in soft terrain [1] [2].

Walking robots, well equipped for traversing rough or soft terrain, also have drawbacks. The time-consuming process of picking up and placing limbs results in slower traverse. In addition, lifting contact points from the ground risks robot instability.

The All-Terrain Hex-Limbed Extra-Terrestrial Explorer (ATHLETE) is a unique mobility system with both walking and driving capabilities. A NASA prototype for lunar exploration, ATHLETE was designed to transport large payloads across highly variable terrain. With a wheel on the end of each articulated limb, ATHLETE can drive on benign terrain and walk when the surface is too soft or rough for driving.

To demonstrate the ATHLETE concept, the Jet Propulsion Laboratory (JPL) has designed and constructed several prototype vehicles, referred to as Software Development Models (SDM). The current demonstration platform is the second-generation ATHLETE prototype, built in 2009 and referred to as SDM-T12 [3] [4].

SDM-T12 consists of a pair of triangular three-limbed platforms called Tri-ATHLETEs which, when joined by a cargo pallet, form the hexagonal six-limbed system shown in Fig. 1. Sized to perform demonstrations at approximately $\frac{1}{2}$ lunar scale,

Figure 1. ATHLETE SDM-T12 DURING FIELD DEMONSTRATIONS AT BLACK POINT LAVA FLOW, AZ, 2010

it stands to a maximum height of just over 4 m and carries a payload of up to 450 kg on Earth. Each limb has 7 degrees of freedom (DOF), six for precise positioning and one redundant pitch actuator to enable each limb to stow compactly.

The Sliding Gait (SGait) algorithm introduced in this paper takes advantage of ATHLETE's capabilities to combine the best features of wheeled driving and legged walking. SGait implements a tripod walking gait which, instead of picking up and placing limbs, slides them along the ground on wheels. This arrangement allows for the stability of driving, with all wheels in continuous contact with the ground, along with the terrain-handling capability of walking, with independent terrain compliance as wheels are repositioned.

BACKGROUND

Many rovers take advantage of articulated joints in a passive suspension system for improving mobility over steep or low-traction terrain. Some examples are JPL's Sample Return Rover (SRR), the Scarab rover from Carnegie Mellon University, and Johnson Space Center's Space Exploration Vehicle (SEV). SRR's articulated "shoulder" joints allow the rover to shift its center of gravity for better balance on steep terrain [5]. Each of SEV's six wheels have both passive suspension and active control over wheel height. Coupled with force feedback, this enables the rover to actively distribute forces for a smoother ride over bumpy terrain [6]. Scarab uses a four-wheeled suspension system with an articulated shoulder joint, similar to SRR, to implement a mobility mode called inching [7]. Inching, similar in concept to SGait, involves using two wheels as stationary anchors while the shoulder and remaining wheels coordinate to progress up sandy slopes.

SGait represents an improvement in capability over these previous efforts. The articulation ability of ATHLETE's active suspension system enables independent repositioning of wheels in any direction. This allows SGait to emulate a walking gait with terrain compliance in any direction, over slopes, and through obstacle-strewn terrain.

CAPABILITIES AND LIMITATIONS OF ATHLETE DRIVING MOBILITY

The ATHLETE concept is feasible for a planetary rover because the ATHLETE mobility system's walking capability allows smaller, lighter wheel actuators. Wheel actuators for JPL rovers with passive suspension systems are designed with sufficient torque and ground pressure to propel half the rover's mass. This provides margin in mobility performance for extracting the vehicle if it encounters unfortunate terrain. In contrast, ATHLETE can pick up and place its wheels, and does not depend on driving mobility for extraction from undesirable terrain. Thus, ATHLETE's wheels can be designed for driving over nominal terrain, with reduced wheel diameters and lighter actuators. The resulting weight savings in the wheel design offsets the mass of the 7-DOF manipulators.

The ATHLETE mobility system has minimal passive compliance. While driving, the tires enable compliance to obstacles smaller than 25% of the wheel diameter. Compliance to larger obstacles or sloping terrain features is accomplished through active control of the limbs. ATHLETE's onboard software runs an active compliance algorithm that uses force feedback to conform to terrain and maintain a level and balanced cargo deck [8].

In 2010, SDM-T12 drove more than 80 km over rolling desert terrain in California and Arizona [9]. On benign terrain, ATHLETE achieves an overall traverse speed of approximately 1 km/hr, but travels more slowly when the terrain is bumpy or sloped. The size and strength of its wheels limits ATHLETE's ability to ascend sloped terrain. In field operations, traversing up slopes has caused wheels to stall.

THE SLIDING GAIT ALGORITHM

Sliding Gait is a mobility mode with characteristics of both walking and driving. Like walking, SGait repositions a subset of limbs while the stationary limbs support the robot's body. Like driving, the wheels stay in contact with the ground and follow the contours of the terrain. In the ATHLETE implementation, the robot's articulated limbs enable coordinated positioning of any wheel along any path, enabling a walking gait.

SGait can traverse with any hexapod walking gait, and the alternating tripod gait has been selected for its time efficiency. In the alternating tripod gait, three limbs provide static support while the other three limbs are repositioned. For a walker, the tripod gait is considered risky on natural terrain, since terrain shifting under a single limb could result in system instability [10]. The SGait algorithm, on the other hand, can safely use an alternating tripod gait because both the sliding tripod and the standing tripod remain in continuous contact with the ground.

The initial implementation of SGait computes a series of

sliding alternating tripod steps along a straight-line path at a commanded heading and distance. The heading is defined in the rover frame as illustrated in Fig. 2. A heading along the X axis of the rover frame, x_R, is defined as 0° and the angle increases clockwise in a right-handed fashion about z_R.

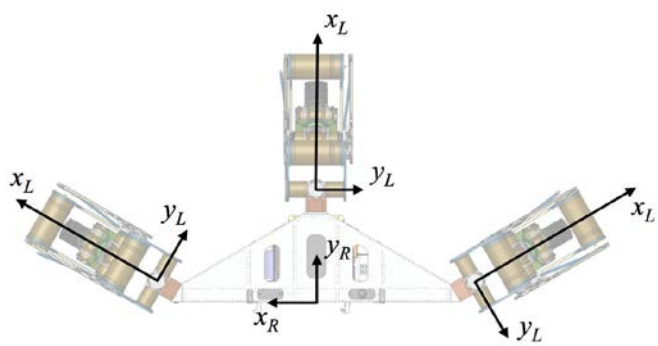

Figure 2. ATHLETE ROVER FRAME AND LEG FRAMES SHOWN ON AN OVERHEAD VIEW OF A TRI-ATHLETE. WHEN MATED IN A SIX-LIMBED SYSTEM, ROVER FRAME ORIENTATION IS MAINTAINED WITH RESPECT TO THE MASTER TRI-ATHLETE, BUT TRANSLATED ALONG $-y_R$ TO THE CENTER OF THE MATED SYSTEM. BOTH COORDINATE FRAMES ARE RIGHT-HANDED, WITH z_R AND z_L POINTING DOWN.

Sliding Gait is built upon an ATHLETE behavior for rolling wheels along the ground while using force feedback to actively comply to natural terrain. To create the sequence of SGait motions, the workspace of each limb is analyzed to determine a maximum step size achievable by all six limbs at the desired heading. A step of this size is then placed within each limb's workspace, defining the extended and retracted positions for each limb in the rover frame. Finally, a series of limb and body motions is constructed to execute a SGait traverse to the commanded distance. The sections that follow present each of these steps in detail.

Because ATHLETE is a NASA prototype, it is designed to be consistent with the computing limitations of space vehicles executing realtime operations. Spacecraft onboard computers typically have limited computational power due to the limited selection of radiation-hardened electronics available. In recognition of these limitations, computationally intensive search algorithms or matrix inversions are avoided when a simple geometric computation will suffice.

Wheel Positioning via Active Rolling

Sliding Gait is enabled by ATHLETE's ability to coordinate wheel and limb motion. Scarab spins wheels freely while inching, using suspension articulation to reduce slip. In contrast, ATHLETE matches wheel rotation to articulation distance, rolling wheels along the ground to specified goal locations, which may be anywhere in the limb's reachable workspace.

Execution of a wheel roll begins with the transformation of the goal position to an (x, y) coordinate in the tool frame, illustrated in Fig. 3. The wheel is steered toward the goal, then commanded to roll a short distance along the tool frame X axis, x_{tool}. Concurrently, the limb is commanded to translate the wheel fork the same distance in the x_{tool} direction. Periodically, at a default rate of just over 2 Hz, the commanded positions of both wheel and limb are updated to a point slightly further along the path. The system redirects to the new via point seamlessly, provided the update rate, speed, and distance are properly matched. These updates continue until the goal position is reached.

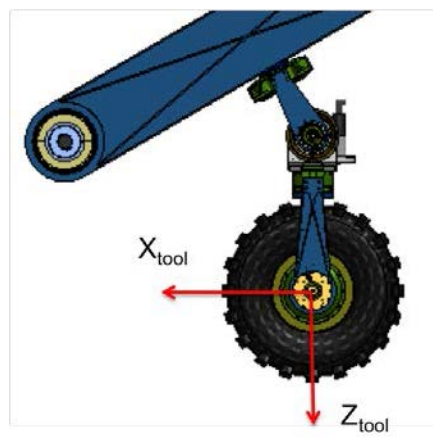

Figure 3. ATHLETE TOOL FRAME. THE FRAME IS RIGHT-HANDED, WITH y_{tool} DIRECTED INTO THE PAGE.

At each update, the sensed wheel and limb positions are compared, looking for mismatches that may be caused by terrain interactions, changes in wheel speed, or other factors. Any difference in position is directly applied to the next via, adjusting the commanded fork position to resynchronize fork and wheel.

Because the wheel is rolled blindly along x_{tool}, slight errors in wheel orientation can result in failure to reach the goal position, particularly over a long distance. To prevent this, the wheel yaw is compared to the goal direction at each update interval. If the wheel direction is out of tolerance, the next via update includes an orientation correction.

Force feedback enables compliance to terrain variations while the wheel is rolling. By default, the onboard algorithm distributes normal loads, in the z_{tool} direction, evenly over all six wheels. At each update interval, the ideal forces on each wheel are calculated based on the limb kinematics. As terrain variations affect actual wheel loading, the deviations in load are sensed and the wheel height is adjusted, following the curvature of the terrain. Wheel height adjustments for each update interval are selected by the same linear interpolation method used in the algorithm for active compliance while driving [8].

Applying force feedback to all wheels results in active com-

pliance of the suspension to the terrain as each motion progresses. Terrain slopes and surface roughness are sensed proprioceptively and continuously accommodated. This feature enables traverse over a wide range of terrain types.

By default, each rolling wheel is controlled to 100% of its ideal load. To aid wheel rolling in particularly soft, steep, or obstacle rich terrains, the operator can reduce the load target for active compliance. This option distributes a larger percentage of rover mass to the standing legs, effectively lowering the surface pressure for the rolling wheels.

Calculating the Maximum Step Size

Because each SGait step is executed via wheel rolling, for which only (x, y) goal coordinates are required, the calculation of maximum step size for SGait traverse uses a planar cross-section of the limb workspace. For each limb, the outer edge of the workspace cross-section is bounded by the horizontal reach of the limb, h_{reach}, rotated around the origin of the leg frame, which is located at the center of the hip yaw joint as shown in Fig. 2. The inner boundary of the workspace is a line at x_{min}, a minimum value of x_L selected ensure a stable supporting stance and avoid the kinematic singularity that occurs when the steering actuator aligns with the hip yaw. In Fig. 4 and Fig. 5, the blue semicircle represents the limb workspace cross-section, and the red line indicates the location of x_{min}.

The workspace size depends on h_{reach}, the radius of the workspace cross-section as shown in blue in figures 4 and 5, which varies with the vertical extension, v_{reach}, of the limb. Because the terrain contour is not modeled, v_{reach} is set to the limb's current z_L position when SGait is invoked, and a vertical margin, v_{marg}, is added to provide for terrain variation during the traverse. With this assumption,

$$h_{reach} = \sqrt{r_{max}^2 - (v_{reach} + v_{marg})^2 + d_{HP}}, \qquad (1)$$

where r_{max} is the maximum extension of the limb from hip pitch to ankle pitch and d_{HP} is the horizontal offset between the leg frame origin and the hip pitch joint.

The circular boundary of the workspace cross-section enables exact calculation of the maximum step size, *maxstep*, for any direction of travel, θ, where *maxstep* is the length of the longest line segment inscribable within the workspace and parallel to the direction of travel. θ is defined in the leg frame as 0° at the leg frame X axis, increasing clockwise in a right-handed manner about z_L, and indicated by the yellow shading in each workspace diagram.

For $-45° < \theta < 45°$,

$$maxstep = \frac{(h_{reach} - x_{min})}{\cos\theta}, \qquad (2)$$

and the maximum step maps into the workspace with one endpoint at $(x_L, y_L) = (0, h_{reach})$, as illustrated by the black arrow in

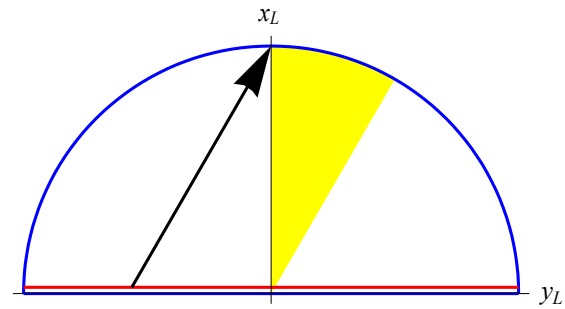

Figure 4. MAXIMUM STEP AT AN ANGLE OF 30° IN LEG FRAME. THE BLUE SEMICIRCLE, WITH RADIUS h_{reach}, REPRESENTS THE BOUNDARY OF THE LIMB WORKSPACE. THE WORKSPACE IS ADDITIONALLY LIMITED BY x_{min}, REPRESENTED BY THE RED LINE.

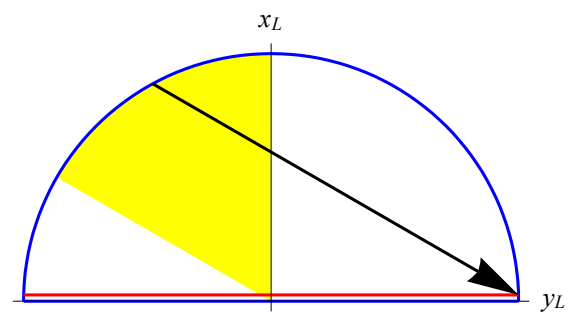

Figure 5. MAXIMUM STEP AT AN ANGLE OF 120° IN LEG FRAME THIS IS EQUIVALENT TO THE MAXIMUM STEP AT -60°, BUT REVERSED IN DIRECTION.

Fig. 4. For all other angles in the range $-90° \le \theta \le 90°$, *maxstep* is the chord length at a radius R from the leg frame origin,

$$maxstep = 2\sqrt{h_{reach}^2 - R^2}, \qquad (3)$$

where

$$R = \frac{x_{min}}{\sin\theta} + \left(\sqrt{h_{reach}^2 - x_{min}^2} - \frac{x_{min}}{\tan\theta}\right)\cos\theta. \qquad (4)$$

In this case the maximum step maps into the workspace with one endpoint at $x_L = x_{min}$ and the associated intersection with the circular workspace boundary, as illustrated by the black arrow in Fig. 5. Note that for $|\theta| > 90°$, the angle is mapped back into the range $-90°$ to $+90°$ with a reversal in step direction. For this reason, an arrowhead is used in the figures to indicate the step direction within the workspace. Fig. 5 illustrates this mapping concept as calculated for $\theta = 120°$.

Because the SGait step size, d_{step}, must be achievable by all six limbs, the maximum step sizes for all limbs are compared and the minimum is selected as d_{step}.

Defining SGait Steps for Six Limbs

With d_{step} selected, a location for the step can be selected within each limb's workspace. The SGait algorithm places the center of the step near a goal position (g_x, g_y) defined in leg frame within the limb workspace, prioritizing g_x over g_y. While the goal position is currently a parameter set by the operator, it provides a hook for further optimization of the step position in the future if desired.

Relocation of the step is performed as a series of geometric transformations. First, a step of length d_{step} is placed with its center at the goal position, (g_x, g_y). The positions of the endpoints, $(e1_x, e1_y)$ and $(e2_x, e2_y)$ are calculated and their position is checked against the boundaries of the limb workspace. If either endpoint is outside a workspace boundary, the position of the step center is adjusted. If the y_L component of the step, Δy, is less than or equal to the sum of $\frac{1}{2}$ the chord length at the X coordinate of each endpoint, i.e.,

$$\Delta y \leq \sqrt{h_{reach}^2 - e1_x^2} + \sqrt{h_{reach}^2 - e2_x^2}, \tag{5}$$

then the step can fit within the workspace at the g_x location, with only a shift in g_y. In this case, the center point of the step is shifted in the y_L direction enough to move the protruding endpoint onto the workspace boundary. For example, if $e1$ is the endpoint out of bounds, the change in center position is

$$\Delta g_y = sign(e1_y)\sqrt{h_{reach}^2 - e1_x^2} - |e1_y| \tag{6}$$

On the other hand, if (5) is not true, and Δy is too large to fit within the workspace at the center location g_x, then the step center must be shifted in both x_L and y_L. The closest position within the workspace is where the step size is equal in length to a chord at the same angle θ. In this case, the center point is moved to the center of the chord, at

$$newg_x = \sin\theta\sqrt{h_{reach}^2 - 0.25d_{step}^2} \tag{7}$$

$$newg_y = -sign(\theta)\cos\theta\sqrt{h_{reach}^2 - 0.25d_{step}^2} \tag{8}$$

The final phase of step placement is eliminating overlap. Overlapping of steps is possible for SDM-T12, since the legs are long relative to the hex dimension, and limb workspaces substantially overlap, as illustrated in Fig. 6. The minimum values for along-track clearance and side clearance of adjacent wheels are x_c and y_c respectively, and are defined in step frame, a coordinate system that shares the rover frame origin but is rotated by the heading angle, θ.

To evaluate the steps for overlap, the step endpoints are transformed into step frame and are checked for overlap with

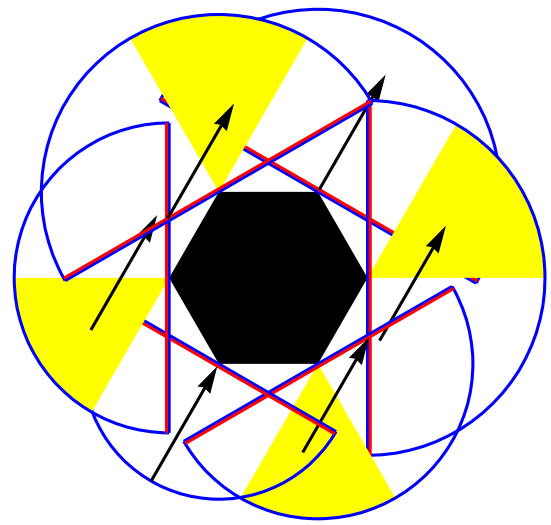

Figure 6. SGAIT STEPS AND WORKSPACES FOR ATHLETE SDM-T12 TRAVERSING AT A HEADING OF 30° DIRECTLY UP A 20° SLOPE. THE SMALLER WORKSPACES REFLECT LONGER VERTICAL EXTENSION IN THE DOWNSLOPE LIMBS.

neighboring steps. If the parallel clearance is insufficient, as determined by

$$|y_n - y_{(n+1)}| < y_c, \tag{9}$$

where y_n and $y_{(n+1)}$ are the y positions of two neighboring steps in step frame, then the steps are checked for along-track overlap. There is overlap if

$$-x_c < x_{nf} - x_{(n+1)b} < 2d_{step} + x_c, \tag{10}$$

where x_{nf} is the step frame x coordinate of the front endpoint of one step and $x_{(n+1)b}$ is the step frame x coordinate of the back endpoint of a neighboring step.

If this is the case, SGait attempts to relocate the outer step to achieve sufficient side clearance, by pushing the step further out via the relocation procedure with a revised (g_x, g_y). If the boundary of the workspace is encountered and clearance is not achieved, the process is repeated, relocating the inner step further in. If workspace limitations prevent the minimum clearance from being achieved, the algorithm fails with an error. Future upgrades to SGait could modify this to retry with shorter step size until a solution is found.

Sequencing the SGait Traverse

With the step endpoints set, SGait next creates the sequence of motions that execute the commanded traverse. Alternating sets of limbs form the tripods for traverse, and the step with maximum x_{nf} identifies the forward tripod.

Because ATHLETE's limb positions are arbitrary at the beginning of the traverse, the starting positions of the rear tripod may be unreachable when fully extended in the initial SGait step. To ensure reachability, the first SGait motion rolls the wheels of the rear tripod to their step midpoints.

Figure 7 illustrates the gait pattern of the SGait traverse. First, the limbs of the front tripod are rolled to the absolute coordinates in rover frame that define their front endpoints. Next, the body is advanced $\frac{1}{2} d_{step}$ in the traverse direction. This is a relative move in rover frame that centers the body over the front tripod, and leaves the rear tripod limbs in their rear endpoint positions in rover frame absolute coordinates. Also during this move, the body height is adjusted to maintain the preferred vertical extensions of the limbs. Third, the rear tripod limbs are advanced to their front endpoints, again using absolute coordinates in rover frame. Finally the body is again advanced $\frac{1}{2} d_{step}$ to center over the rear tripod, completing the sequence with the front tripod limbs at their rear endpoint positions. This set of motions is repeated until less than $\frac{1}{2} d_{step}$ remains in the commanded traverse distance.

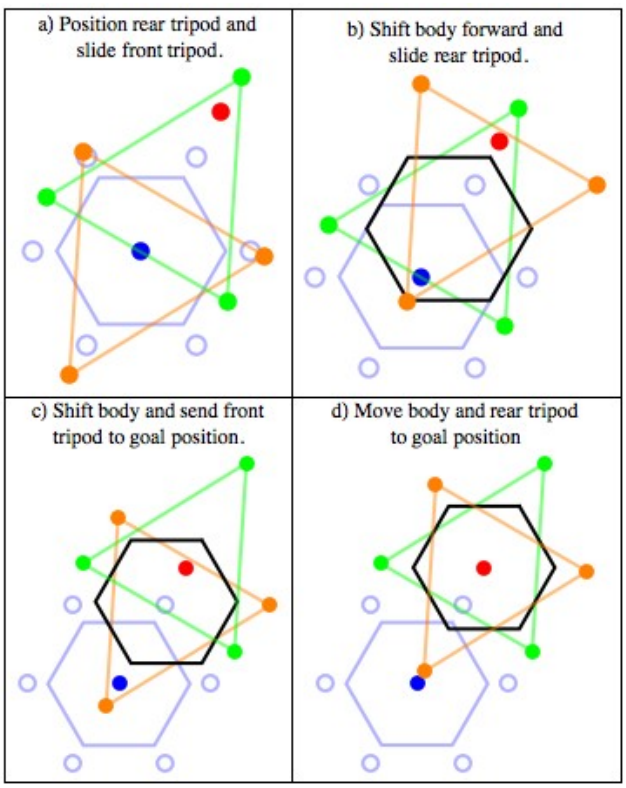

Figure 7. ILLUSTRATION OF 3.5 M SGAIT TRAVERSE AT A HEADING OF 30° DIRECTLY UP A 20° SLOPE. THE BLUE DOT AND OUTLINE SHOW ATHLETE'S STARTING POSITION AND THE RED DOT REPRESENTS THE END OF TRAVERSE. THE HEXAGONS REPRESENT ATHLETE'S BODY, AND THE GREEN AND ORANGE TRIANGLES REPRESENT THE FRONT AND REAR TRIPODS, RESPECTIVELY.

For the final step, all position commands are adjusted such that ATHLETE will finish in the correct position with the body centered over both tripods. First, the tripod currently at the back of its step is moved along its step path a distance of $\frac{1}{2} d_{step} + d_{end}$ from its rear endpoints, where d_{end} is the distance remaining to the end of the traverse. Next the body is shifted by distance d_{end}, with the corresponding height adjustment, to center over this tripod. Finally, the remaining tripod is moved d_{end} along its step path, leaving ATHLETE in a symmetric pose with the body center at the commanded distance from the starting position.

RESULTS OF PRELIMINARY TESTING

In September 2010, during field testing at Black Point Lava Flow in Arizona, the team tested wheel rolling with active terrain compliance. The effectiveness of the behavior was demonstrated and it was subsequently used during traverse operations for adjusting wheel positions on sloped terrain.

Figure 9 shows the rover frame positions of wheel 5 as it traversed the berm shown in Fig. 8 in a sequence of wheel rolling and body shifting moves approximating a SGait traverse. As Fig. 9 illustrates, wheel 5 traces the contour of the berm with each subsequent wheel rolling maneuver. This demonstrates the capability of the force feedback system to conform to rough terrain proprioceptively as the wheels are rolled to each new position. Because this active terrain compliance is embedded in the wheel rolling behavior, each wheel similarly conforms to the local terrain while sliding, enabling SGait traverse over a wide variety of terrain types without explicit mapping or planning.

The contact forces in the normal, z_{tool}, and along-track, x_{tool} directions during the same period are shown in Fig. 10. Note that the variation in the forces is within +/- 500 N, which is within the observed hysteresis of the force estimator for SDM-T12. This illustrates the effectiveness of the active compliance algorithm in maintaining a constant load distribution on wheel 5 as the berm is traversed.

CONCLUSIONS AND FUTURE WORK

Conclusions

The SGait algorithm for ATHLETE is a mobility mode that represents a hybrid of both driving and walking capabilities. With active loading management and a walking gait, SGait has the potential to enable a wheeled system to traverse soft, hilly, or obstacle-rich terrain beyond the capabilities of a standard passive suspension rover. Though similar to walking, SGait keeps all wheels in contact with the ground throughout traverse, making it more time efficient and conservatively stable than a pure walking gait.

The wheel rolling behavior upon which the SGait traverse is built has been implemented in the onboard software for the ATHLETE SDMs. In field testing, wheel rolling with active terrain compliance has been proven effective and capable.

Figure 8. ATHLETE SDM-T12 TRAVERSING A BERM. THE LEADING LIMB, SHOWN NEAR THE TOP OF THE BERM, IS LEG 5.

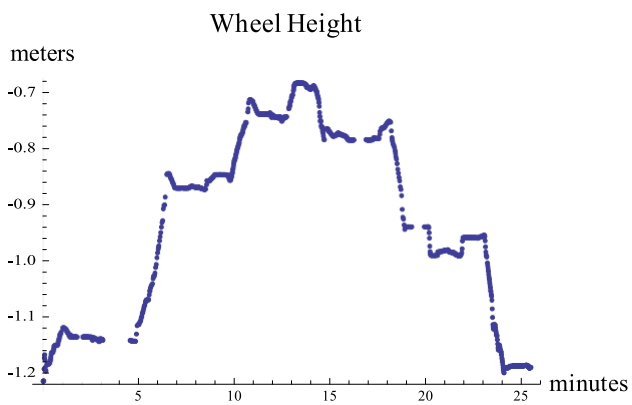

Figure 9. POSITION OF WHEEL 5 IN ROVER FRAME, z_R, AS IT IS ROLLED OVER THE BERM. BECAUSE z_R INCREASES WITH EXTENSION DOWNWARD, THE POSITIONS ARE PLOTTED AS $-1 * z_R$ SO THE CONTOUR OF THE BERM APPEARS IN A RECOGNIZABLE ORIENTATION.

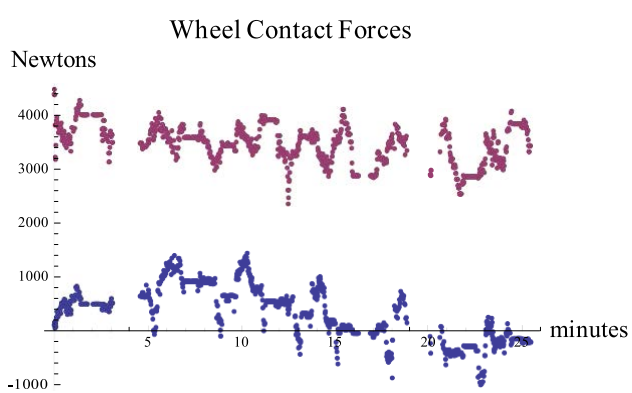

Figure 10. FORCES ON WHEEL 5 WHILE ROLLING OVER THE BERM. THE UPPER DATA SET SHOWS NORMAL FORCES, ALONG z_{tool}, AND THE LOWER DATA SET SHOWS THE DRIVE DIRECTION FORCES, ALONG x_{tool}.

Future Work

Over the coming months, the SGait algorithm will be implemented in ATHLETE's onboard software and undergo a battery of characterization tests in the JPL Mars Yard. In these tests, the slope climbing performance of SGait will be compared to the performance of active driving on the same slopes.

Future improvements on the SGait algorithm will be influenced by the results of testing. They may include the implementation of SGait for arcing paths and relaxing the requirement for a level cargo deck to allow access to steeper slopes. Other improvements, such as optimization of vertical margin, step placement, or body height may be investigated if required for traverse performance.

ACKNOWLEDGMENT

The research described in this paper was carried out at the Jet Propulsion Laboratory, California Institute of Technology, under a contract with the National Aeronautics and Space Administration. ATHLETE development at JPL is led by Principal Investigator Brian Wilcox and is conducted under the Human-Robot Systems Project led by Rob Ambrose of JSC with funding from the NASA Office of Chief Technologist, Game Changing Division.

REFERENCES

[1] Arvidson, R. E., et al. (2010), Spirit Mars Rover Mission: Overview and selected results from the northern Home Plate Winter Haven to the side of Scamander crater, *J. Geophys. Res.*, 115, E00F03, doi:10.1029/2010JE003633.

[2] Arvidson, R. E., et al. (2011), Opportunity Mars Rover mission: Overview and selected results from Purgatory ripple to traverses to Endeavour crater, *J. Geophys. Res.*, 116, E00F15, doi:10.1029/2010JE003746.

[3] Wilcox, B. H., "ATHLETE: A Cargo-Handling Vehicle for Solar System Exploration," *IEEE Aerospace Conference*, 2011.

[4] Heverly, M., Matthews, J., Frost, M., and McQuin, C., "Development of the Tri-ATHLETE Lunar Vehicle Prototype," *Proceedings of the 40th Aerospace Mechanisms Symposium*, May 2010.

[5] Iagnemma, K., Rzepniewski, A., Dubouwsky, S., and Schenker, P., "Control of Robotic Vehicles with Actively Articulated Suspensions in Rough Terrain," *Autonomous Robots*, 14, pp. 5-16, 2003.

[6] Bluethmann, B., Herrera, E., Hulse, A., Figuered, J., Junkin, L., Markee, M., and Ambrose, R. O., "An Active Suspension System for Lunar Crew Mobility," *IEEE Aerospace Conference*, 2010.

[7] Moreland, S. J., Skonieczny, K., and Wettergreen, D., "Inching Locomotion for Planetary Rover Mobility," *IEEE Aerospace Conference*, March, 2011.

[8] Townsend, J., Biesiadecki, J., and Collins, C., "ATHLETE

Mobility Performance with Active Terrain Compliance," *IEEE Aerospace Conference*, 2010.

[9] Townsend, J., "ATHLETE Mobility Performance in Long-Range Traverse," *AIAA Space 2011 Conference and Exposition*, September, 2011.

[10] Wettergreen, D., "Robotic walking in natural terrain: Gait planning and behavior-based control for statically-stable walking robots," Ph.D. Thesis, Carnegie Mellon University, 1995.